

# Design-Oriented Analysis and Performance Evaluation of Single Phase AC-DC Buck Boost Converter

Jayahar\* R. Ranihemamalini\*\* and K.Rathnakannan\*\*\*

**Abstract :** This research work presents the Power Factor Correction (PFC), harmonics elimination of single phase Buck-Boost Converter (BBC) working in Continuous Conduction Mode (CCM) by using both Linear Current Controller (LCC) and Proportional-Integral (PI) Controller is used. The Integral Controller is used as voltage control loop and LCC is working as current loop for power factor correction. The proposed controllers have advantages such as robustness, less harmonics and good PFC when there are large variations in line voltage and the load. The PI controller is using for state space average modeling of BBC. The simulation of the given system with its control model is implemented in MatLab/Simulink. The theoretical and simulation numerical results shows a nearly unity power factor can be attained and there is almost no change in power factor when the line frequency is at various ranges. Experimental and simulation results are conformed the analysis and verified the feasibility of the proposed converter topology.

**Keywords :** PFC, Buck-Boost converter, Linear Current Mode Control and PI controller.

## 1. INTRODUCTION

The most simple from the  $H_{\infty}$  algorithm and applied to the controller and the experimental results performed better than the PID controller [1]. Ac-Dc buck-boost converter is analyzed to compare with the conventional buck-boost converter.[2]. Recently, the PFC techniques have received with more attained and number of new techniques is proposed [3-5]. The several current control techniques are researched in the literature for boost and cuk single phase PFC rectifiers [6-10]. The important feature of LCC, as compared with average current mode control, is that LCC uses a high gain, wide bandwidth Current Error Amplifier (CEA) to force the average of current within the converter, typically the inductor current and follow the demanded current reference with very small error, as a controlled current source. Advantages of LCMC is large noise margin, no requirement for additional slope compensation, easy current limit consideration, good voltage and current regulation, simple compensation, good behavior in both continuous and discontinuous inductor current modes, and has inherent input voltage and output voltage feed-forward properties. All this is achieved with only a slight increase in complexity over earlier schemes [8]-[9].

LCMC is typically a two loop control method (inner loop, current; outer loop, voltage) for power electronic converters. Many of these applications have been in the higher switching frequency, lower power segment (up to 10kW, at 20 kHz and above), but this is changing. A 30kW three phase inverter using analog LCMC has been reported [7]. The regulation of output voltage of PFC boost converter using PI controller at the outer loop has been reported [13]-[14].

\* Research Scholar, Department of EEE J N T University,Kakinada, India E-mail:jayahar2003@yahoo.co.in

\*\* St.Peters College of Engineering & Tech. Chennai, India E-mail: ranihema@yahoo.com

\*\*\* Anna University, Chennai, India. E-mail:ckrkannan@yahoo.co.in

The simple models of power converters are usually obtained from state-space averaging and linearization techniques; these models may then be used for classical control design [15]-[17].

Therefore in this paper, we propose a PFC BBC to regulate the output voltage/supply current by using both PI controller at the outer loop and the LCMC at inner loop. The state-space average model for BBC is derived at first and used for designing the PI controller.

In section II, the circuit description and mathematical model of PFC Converter. The design of PI controller and LCMC is presented in section III. Simulation results of system are discussed in section IV. The paper ends with some conclusions in section V.

## 2. CIRCUIT DESCRIPTION AND MATHEMATICAL MODEL OF PFC BBC

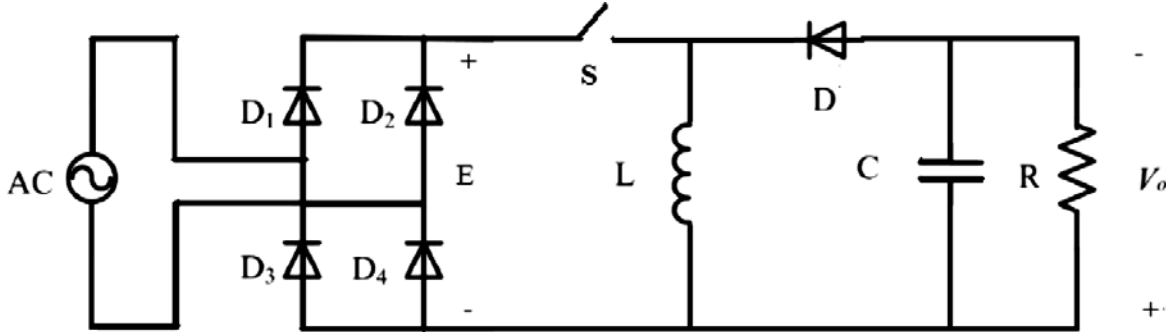


Figure 1: (a) The topology of the PFC B-B Converter

The circuit topology is shown in Fig. 1, and it is constructed by the uncontrolled diode bridge, followed by a BBC. It consists of AC input supply voltage, inductor  $L$ , capacitor  $C$ , power switch  $S$  ( $n$ -channel mosfet), diode  $D$  and load resistance  $R$ . It allows the output voltage to be higher or lower than the input voltage, based on the duty ratio  $d$ . In the circuit there are two storage elements inductor and capacitor. It is customary and convenient to take the inductor current and the capacitor voltage as state variables. Each switching stage can be represented by a corresponding circuit topology.

The voltage transfer gain of BBC is

$$\frac{V_o}{E} = \frac{d}{(1-d)}$$

and it's the corresponding current transfer gain is

$$\frac{I_o}{I_{in}} = \frac{d}{(1-d)}$$

In the on-duration circuit configuration, the switch is conducting and diode is not conducting. The system state equations describing the on-interval circuit configuration is describing by

$$\begin{aligned} \frac{di_L}{dt} &= \frac{E}{L} \\ \frac{dV_c}{dt} &= -\frac{1}{RC} V_c \end{aligned}$$

$$\begin{bmatrix} \frac{di_L}{dt} \\ \frac{dV_c}{dt} \end{bmatrix} = \begin{bmatrix} 0 & 0 \\ 0 & -\frac{1}{RC} \end{bmatrix} \begin{bmatrix} i_L \\ V_c \end{bmatrix} + \begin{bmatrix} \frac{1}{L} \\ 0 \end{bmatrix} E$$

In the off-duration circuit configuration, the switch is opened and the diode is conducting. The system equations for the off-circuit topology are given as

$$\begin{aligned}\frac{di_L}{dt} &= -\frac{V_c}{L} \\ \frac{dV_c}{dt} &= \frac{1}{C}i_L - \frac{1}{RC}V_c \\ \begin{bmatrix} \frac{di_L}{dt} \\ \frac{dV_c}{dt} \end{bmatrix} &= \begin{bmatrix} 0 & -\frac{1}{L} \\ \frac{1}{C} & -\frac{1}{RC} \end{bmatrix} \begin{bmatrix} i_L \\ V_c \end{bmatrix} \quad \dots(2)\end{aligned}$$

By using the state-space averaging model the system model can be written as [14]-[15]

$$A = A_{on}d + A_{off}(1-d)$$

$$B = B_{on}d + B_{off}(1-d)$$

$$\begin{bmatrix} \frac{di_L}{dt} \\ \frac{dV_c}{dt} \end{bmatrix} = \begin{bmatrix} 0 & \frac{-1+d}{L} \\ \frac{1-d}{C} & -\frac{1}{RC} \end{bmatrix} \begin{bmatrix} i_L \\ V_c \end{bmatrix} + \begin{bmatrix} \frac{d}{L} \\ 0 \end{bmatrix} E$$

### 3. DESIGN OF PI CONTROLLER AND LINEAR CURRENT CONTROLLER

#### A. Design PI Controller Design

The PI controller is designed to ensure the specifying desired nominal operating point for PFC BBC, then regulating it, so that it stays very closer to the nominal operating point in the case of sudden disturbances, set point variations, noise, modeling errors and components variations.

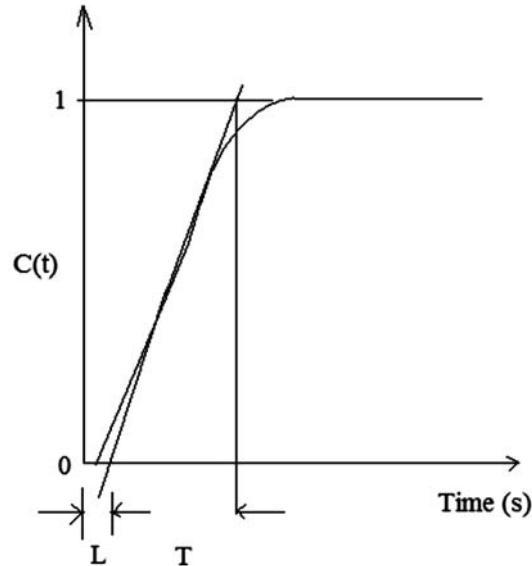


Fig. 2. S- Shaped curve of step response of BBC.

The PI controller settings proportional gain ( $K_p$ ) and integral time ( $T_i$ ) are designed using Zeigler – Nichols tuning method [13]-[14] by applying the step test to (3) to obtain S – shaped curve of step response of BBC. From the S-shaped curve of step response of BBC may be characterized by two constants, delay time L and time constant T. The delay time and time constant are determined by drawing a tangent line at the inflection point of the S-shaped curve and determining the intersections of the tangent line with the time axis and line output response  $c(t)$  as shown in Fig. 2. Ziegler and Nichols suggested to set the values of  $K_p = 0.036$  and  $T_i = 0.016s$  according to the Table I.

The PI controller optimal setting values ( $K_p$  and  $T_i$ ) for PFC BBC are obtained by finding the minimum values of integral of square of error (ISE), integral of time of square of error (ITAE) and integral of absolute of error (IAE), which is listed in Table II. The designed PI controller is used regulate the output voltage of PFC BBC.

**Table 1**  
**Ziegler- Nichols Tuning Rules**

Type of controller	$K_p$	$T_i$	$T_d$
P	T/L	$\infty$	0
PI	0.9T/L	L/0.3	0
PID	1.2T/L	2L	0.5L

**Table 2**  
**Simulated Results Of Minimum Values Of ISE, IAE, ITAE And Optimal Setting Values Of  $K_p$  And  $T_i$**

ISE	IAE	ITAE	$K_p$	$T_i$ (s)
2.366	0.1876	0.001657	0.01324	0.0122

**B. Block Diagram**

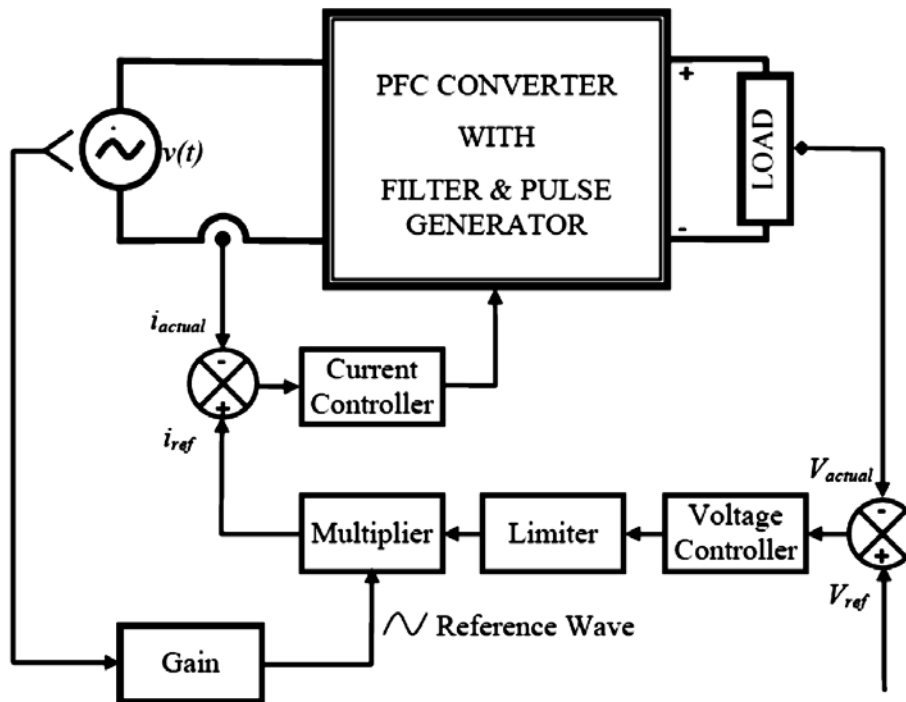


**Figure 3: Block diagram of buck-boost converter**

In Fig.3 shows the block diagram of buck-boost converter, Here the PI controller output and full bridge diode rectifier output are applied to multiplier. Now, multiplier multiplies the both signal to form the modulating signal. This modulating signal and ramp function are applied to summer. Its sums the both signal to form reference current. Then reference current is compared to feedback current to form PWM pulse to control the switch S. The output voltage can be varied by changing the duty cycle. In Fig.4 shows the feedback current is compared with reference sinusoidal waveform is remain between the maximum and minimum values of  $i_{ref}$  [3]. The advantages of LCMC over the inductor average current and hysteresis current controllers as follows.

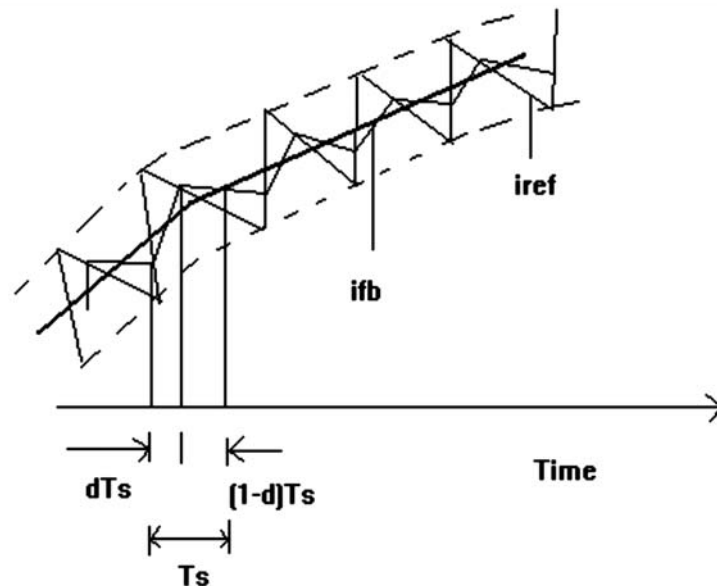


Figure 4: Waveforms of  $i_{fb}$  and  $i_{ref}$

Average current tracks the reference current with high degree of accuracy. This is especially important in high power factor converters.

Slope compensation is not required, but there is a limit to loop gain at switching frequency in order to achieve stability.

Noise immunity is excellent.

#### 4. SIMULATION RESULTS

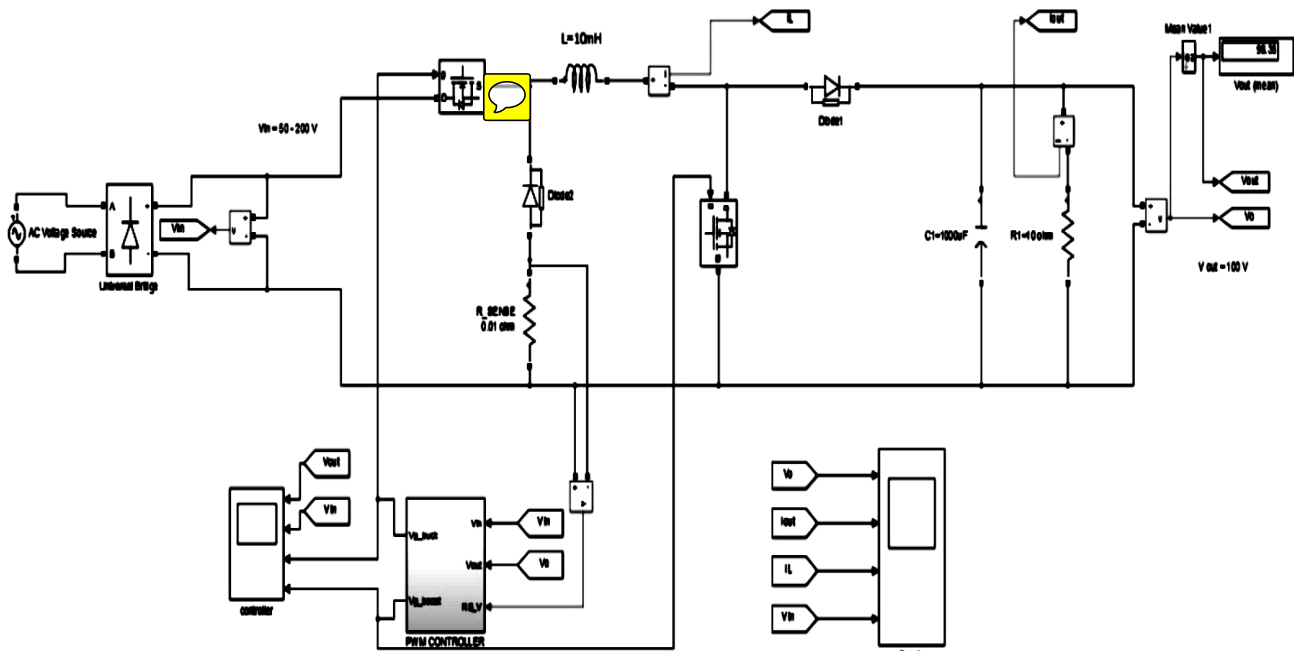


Figure 5: PFC BBC with Linear current and PI controllers

The simulation results of PFC BBC with HCMC and PI controller is used in this section. The single phase PFC BBC with proposed controllers is shown in Fig.5. The nominal input voltage is 50Hz with the RMS value 110V, input inductor  $L_{in} = 70\mu\text{H}$ , inductor  $L = 700\text{mH}$ , capacitor  $C = 760\mu\text{F}$ , the output load range  $R = 100\text{ohm}$  to  $200\text{ohm}$ , the desired output voltage is 200V and the line frequency is 50Hz. The performances of HCMC and PI controller for PFC BBC are evaluated in MatLab/Simulink.

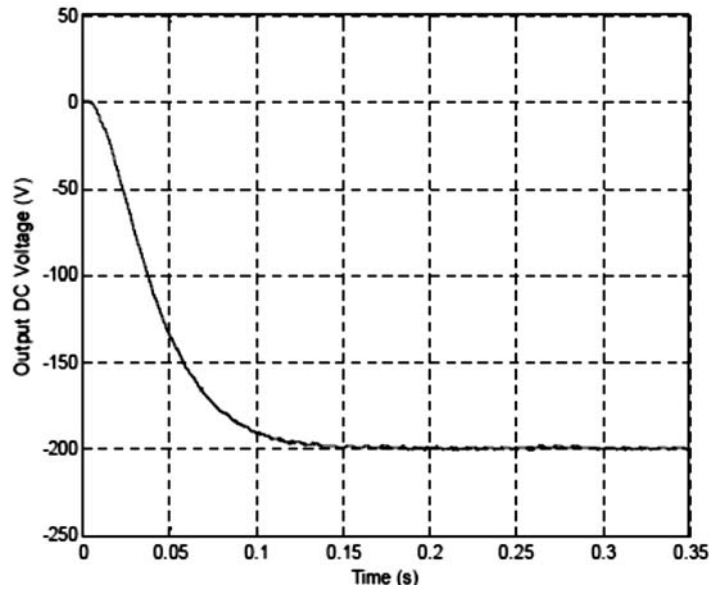


Figure 6: Waveform of the output voltage with constant load  $R = 100 \text{ ohm}$

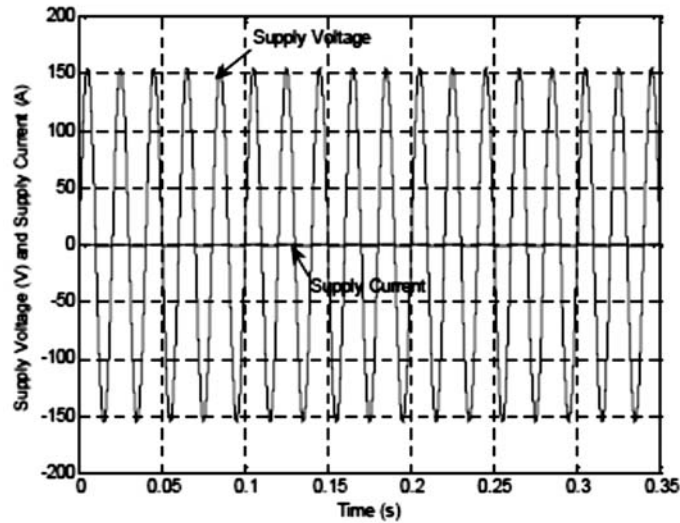


Figure 7: Waveforms of the supply voltage and supply current when  $R = 100 \text{ ohm}$

Under constant load operation, the waveform of the output voltage is obtained as shown in Fig.6. In steady state, the output voltage variation is not more than  $\pm 1.5$ . The input current and voltage waveforms are shown in Fig.7. The input current waveform is almost in phase with the input voltage. From the harmonic spectrum analysis of input current in Fig.8, the Total Harmonic Distortion (THD) is almost up to 9.64%.

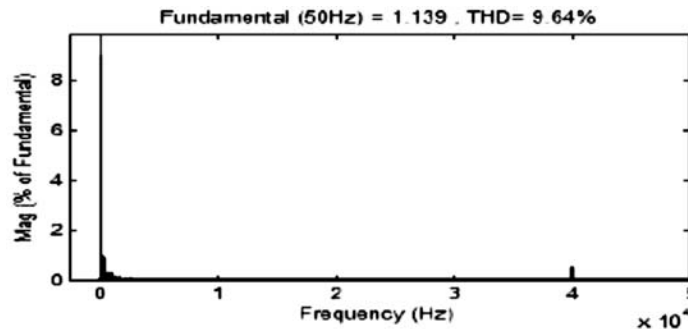


Figure 8: Frequency domain analysis of input current when  $R = 100 \text{ ohm}$

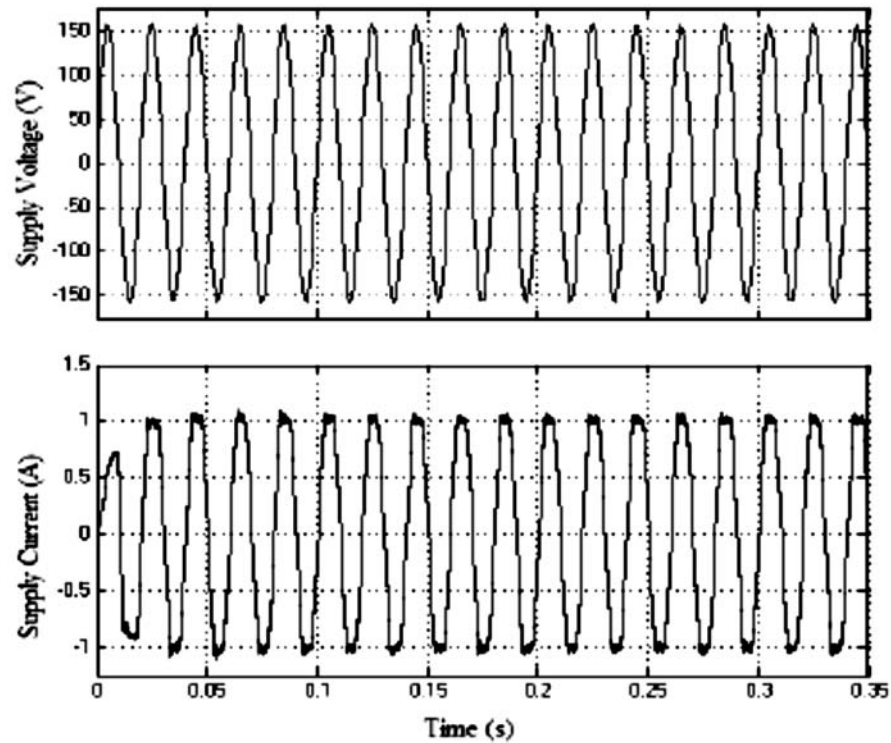


Figure 9: Zoomed waveforms of the supply voltage and supply current when  $R = 100 \text{ ohm}$

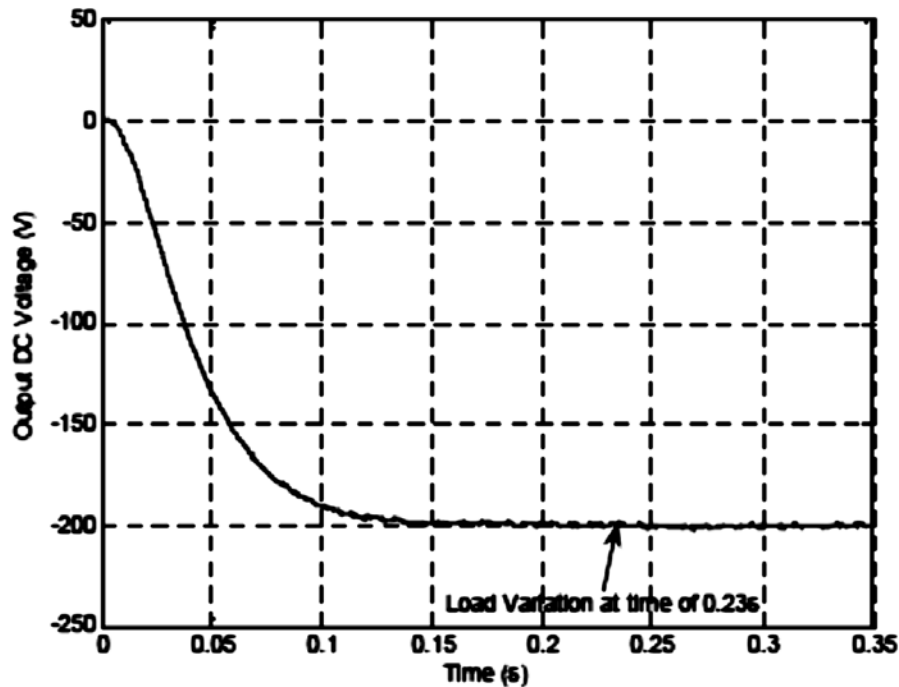


Figure 10: Waveform of output voltage with load change from  $100 \text{ ohm}$  to  $200 \text{ ohm}$  at  $0.23\text{s}$

The zoomed waveform of input current and voltage waveforms are shown in Fig.9. The input current waveform is in phase with the input voltage. From this figure it clearly found that, the power factor nearly unity. When the load changes from  $100 \text{ ohm}$  to  $200 \text{ ohm}$  at  $0.23\text{s}$ , the waveform of the output voltage is shown in Fig. 10, the transient output voltage varies less than  $1\text{V}$  and it can attain stable within  $0.01\text{s}$ , but the ripple is low when the load is larger with designed PI controller. The waveforms of the input current and voltage are shown in Fig.11. It can be seen that the response of the input current is attained stable within two switching cycles under load variations with designed LCMC.



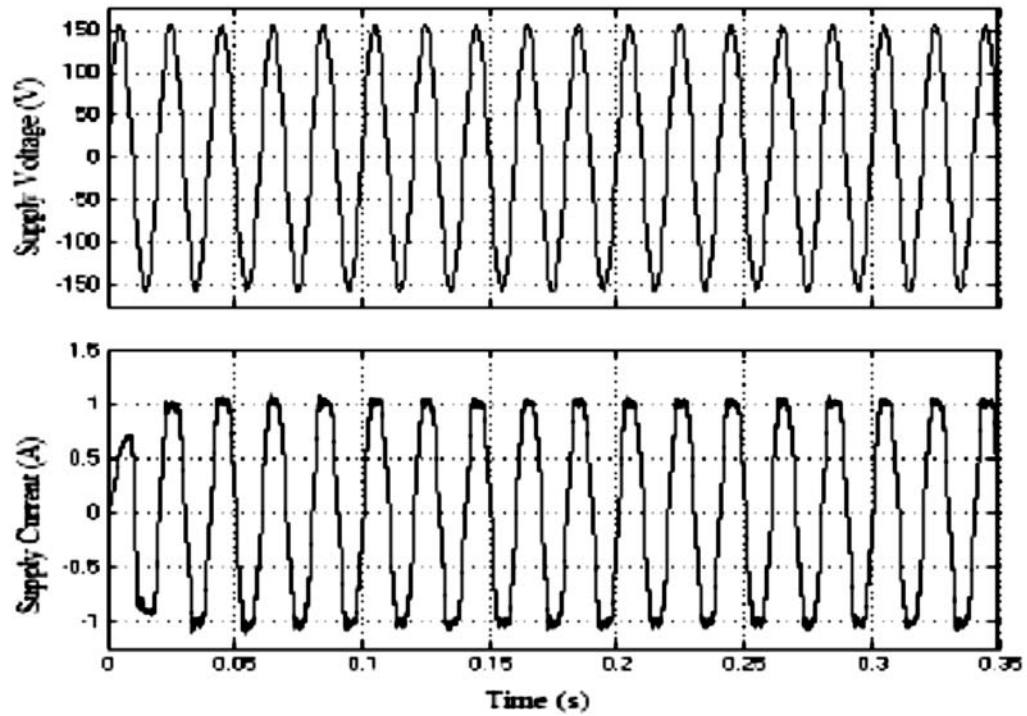


Figure 11: Waveforms of input current and voltage with load change from 100 ohm to 200 ohm at 15s.

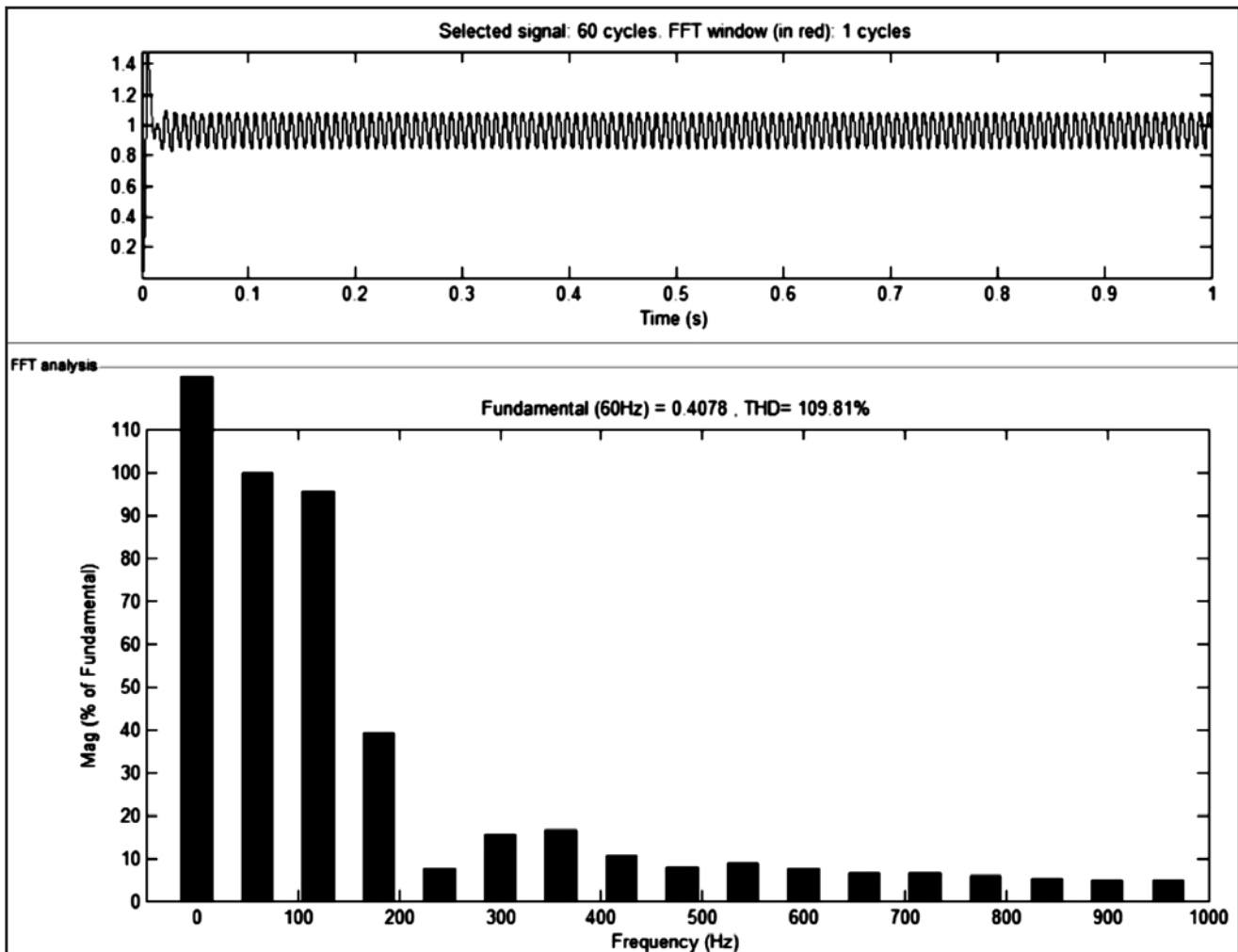


Figure 12: THD comparisons under different line frequencies



## 5. EXPERIMENTAL RESULTS

The specification of experimental model is same as the simulation model specification. The nominal input voltage is 50Hz with the RMS value 110V, input inductor  $L_{in} = 70\mu\text{H}/15\text{A}$  (Ferrite Core), inductor  $L = 700\text{mH}/15\text{A}$  (Ferrite Core), capacitor  $C = 760\text{Mf}/440\text{V}$  (Electrolytic type), the output load range  $R = 100\text{ohm}$  to  $200\text{ohm}$ , the desired output voltage is  $200\text{V}$ , the line frequency is  $50\text{Hz}$ , SIRFN 540 (MOSFET) and FR306 (Diode).

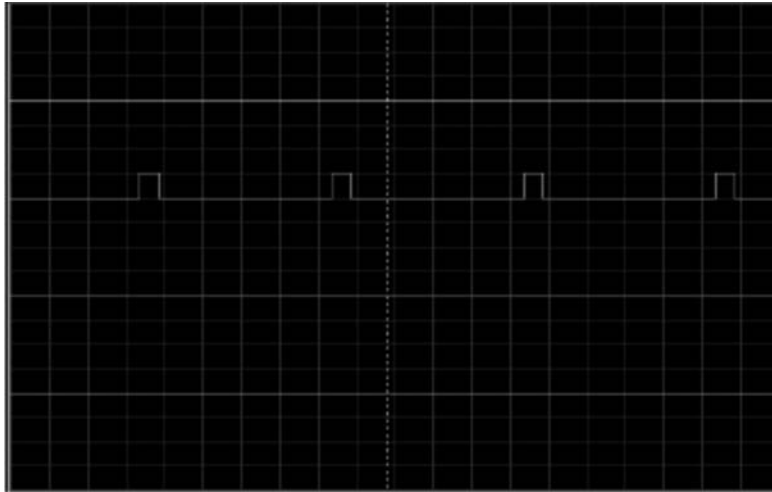


Figure 13: Waveforms of input voltage with load change from 100 ohm to 200 ohm

Fig. 13 shows the input voltage and current with load change from 100 ohm to 200 ohm. From this waveforms it is clearly identified that, there is no fluctuation in input current and voltage using the proposed control scheme.

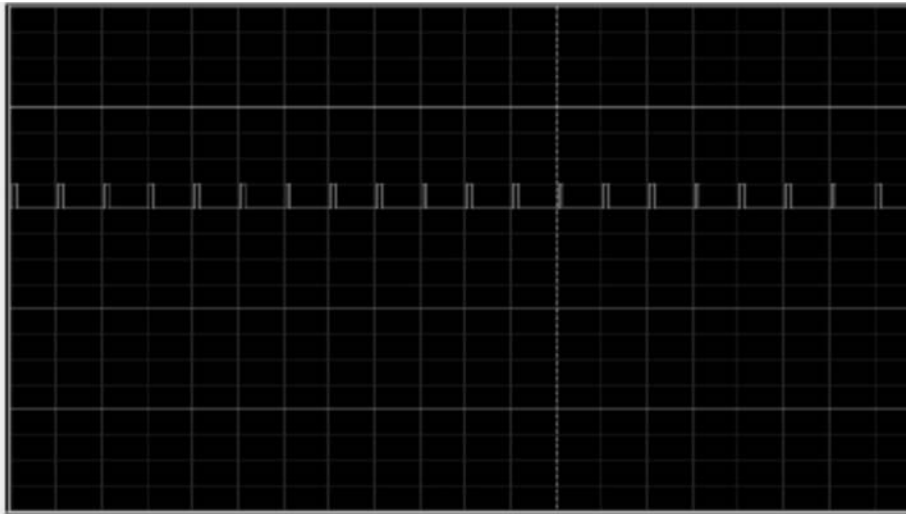


Figure 14: Waveforms of out current and voltage with load change from 100 ohm to 200 ohm

Fig. 14.shows the output voltage and current with load change from 100 ohm to 200 ohm. From these waveforms it is clearly identified that, there is no deviation in output current and voltage using the proposed control scheme. Fig. 15 shows the analog implementation of LCMC with components details. Low voltage range of output is obtained by using potential divider circuit. The PI controller was implemented using LM324, capacitor and feedback resistance. PI controller output and rectified output signals are multiplied by using multiplier AD 633. After the multiplied output signal and ramp signal (NE 555) is summed. The output signal of this operational amplifier is the reference current for feedback inductor current. Both signals are compared using LM311 and generate the pulse width modulation pulse. MCT 2E and transistors is act as an opto-coupler and driver circuit for the MOSFET.

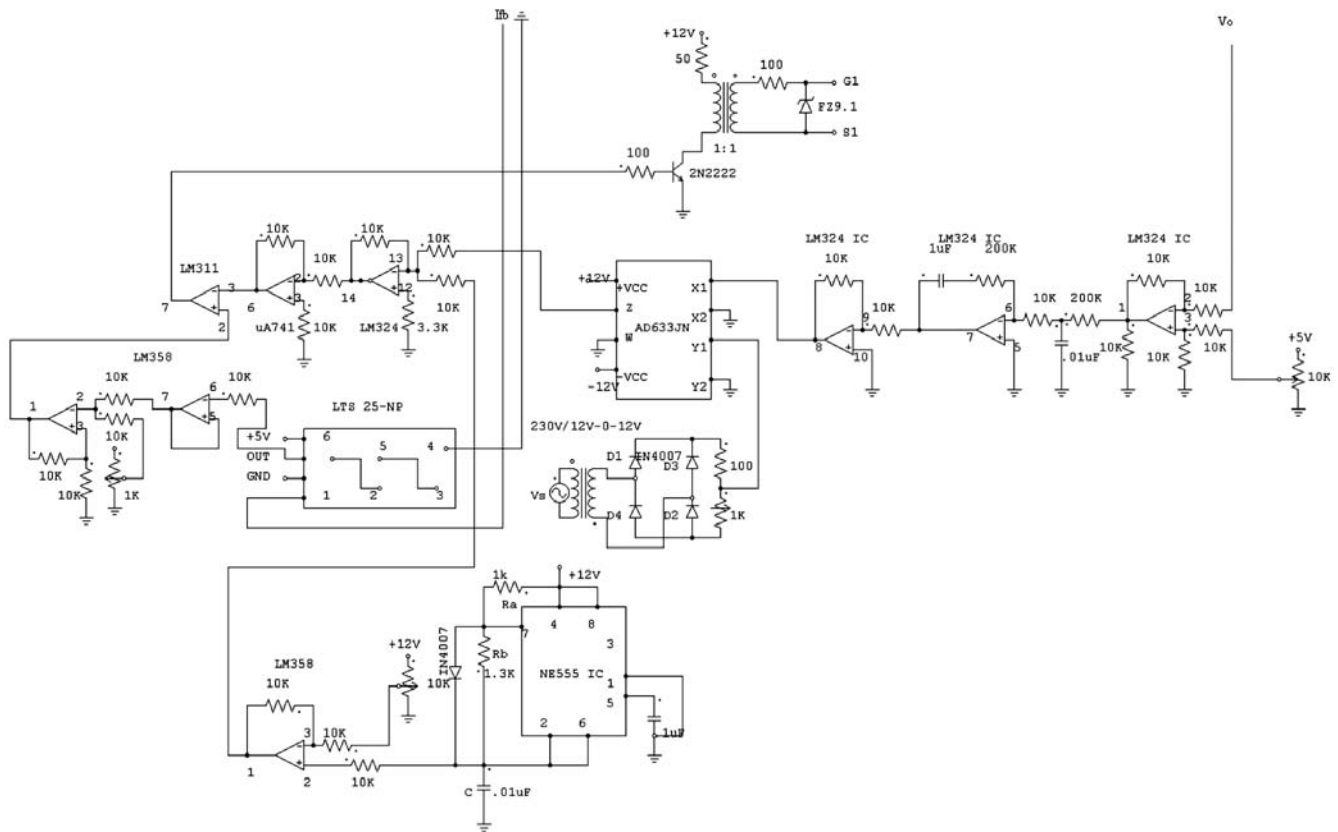


Figure 15: Analog implementation of LCMC

## 6. CONCLUSION

The design of proposed controllers for PFC BBC has been successfully demonstrated and implemented in real time. The input current and harmonics are regulated by inner loop of LCMC, which has the advantages over the inductor average current mode and hysteresis current controllers such as the robustness when there are large variations in line voltage and output load. The PI controller is implemented at outer loop, which produce better performance of output voltage regulation under different conditions. Moreover, this LCMC is advantageous compared to Average current mode controller in the application when the line frequency is changing largely. In addition, the given technique offers definite benefits over the conventional boost converter and it is easy to implement, and get sinusoidal input current from AC source for any DC output voltage condition. The simulation and experimental results reached the theoretical analysis and thus verified the feasibility of the proposed convertor topology.

## 7. REFERENCES

1. Wilmer Hernandez, "Robust control applied to improve the performance of a buck-boost converter" WSEAS Transactions on circuits and systems, volume7, June 2008.
2. Dong-Kurl Kwak, Bong-seob Lee, "A study on Novel Buck-Boost Ac-Dc converter of high performance by partial resonance technique" 7<sup>th</sup> international conference on power electronics, IEEE 2008.
3. W.Guo and P.K Jain "A low frequency ac to high frequency ac inverter with build-in power factor correction and soft switching" IEEE Transactions on P.E, volume-19, March 2004.
4. S.Busio, "Design of a robust voltage controller for a buck-boost converter using  $\mu$ -synthesis, IEEE Transaction on control systems Technology, 1999.
5. L.SYang, T.J.Liang, "Analysis and design of a novel three phase AC-DC buck-boost converter" IEEE transactions on power electronics, May 2008.

6. J. Sun, W. C. Wu, and R. Bass, "Large-signal characterization of single phase PFC circuits with different types of current control," in Proc. IEEE Appl. Power Electron. Conf. (APEC'98), 1998, pp. 655-661.
7. C. Zhou and M. M. Jovanovic, "Design trade-offs in continuous current mode controlled boost power-factor correction circuits," in Proc. HFPC'92, 1992, pp. 209-220.
8. L. H. Dixon, "Average current-mode control of switching power supplies," in *Unitrode Power Supply Design Handbook*. New York: Mc-Graw-Hill, 1990.
9. J. B. Williams, "Design of feedback loop in unity power factor ac to dc converter," in Proc. PESC'89, 1989, pp. 959-967.
10. K. Smedley and S. Cuk, "One-cycle control of switching converters," in Proc. IEEE PESC'91, 1991, pp. 814-820.
11. Fraser, M. E., and Manning, C. D., "Performance of Average current Mode Controlled PWM Inverter with High Crest Factor Load", *Power Electronics and Variable Speed Drives*, 26-28 October 1994, conference Publication No. 399, IEE, pp. 661-666.
12. L. Guo, J. Y. Hung and R. M. Nelms, "Design and implementation of a digital PID controller for a buck converter," Proceedings of the 36th Intersociety Energy Conversion Engineering Conference, July/August (2001), Vol. 1, pp. 187-192.
13. H. Mingzhi and X. Jianping, "Nonlinear PID in Digital Controlled Buck Converters", Applied power electronics conference APEC 2007, 25 Feb-1 March (2007), Anaheim CA USA, pp. 1461-1465.
14. A. J. Foreyth and S. V. Mollov, "Modeling and control of Dc-Dc converters", IEEE Power Engineering Journal, Vol. 12 no. 5, (1998), pp 229-236.
15. Mahdavi, A. Emadi, H. A. Toliyat, "Application of State Space Averaging Method to Sliding Mode Control of PWM DCDC Converters," IEEE Industry Applications Society Annual Meeting New Orleans, Louisiana, October 5-9, (1997), pp. 820-827.
16. Y. C. Ji and M. W. Shan, "A novel three phase AC/DC converter without front-end filter based on adjustable triangular-wave PWM technique," IEEE Trans. Power Electronics, March-1999.
17. B. Singh, B. N. Singh, A. Chandra, and D. P. Kothari, "A review at single Phase improved Power quality Ac-Dc converters, IEEE Trans. Industrial Electronics, Oct, 2003.